Phase Transformations in a Cu-14.2Al-7.8Ni Alloy

C.H. CHEN and T.F. LIU

In the as-quenched condition, the microstructure of the Cu-14.2 wt pct Al-7.8 wt pct Ni alloy was $D0_3$ phase containing extremely fine L–J precipitates with two variants. The L-J precipitate has an orthorhombic structure with lattice parameters $a = 0.413$ nm, $b = 0.254$ nm and $c = 0.728$ nm, which was a new phase found firstly by the present workers. The orientation relationship between the L-J phase and the matrix is $(100)_{L\text{-}J}//(0\bar{1}1)_m$, $(010)_{L\text{-}J}//(1\bar{1}\bar{1})_m$ and $(001)_{L\text{-}J}//(211)_m$. The rotation axis and rotation angle between two variants of the L-J phase are [021] and 90 deg. When the alloy was aged at 500 °C for short times and then quenched, γ_2 particles started to precipitate within the $D0_3$ matrix at the aging temperature and the remaining $D0_3$ matrix would transform to γ_1' martensite during quenching. This is similar to that observed by other workers in a Cu-14Al-4Ni alloy. However, when the alloy was aged at 500 °C for longer times, the remaining $D0_3$ matrix would transform to a mixture of ($B2 + \alpha$) phases. This feature has never been observed by other workers in the Cu-Al-Ni alloys.

I. INTRODUCTION

PHASE transformations in the Cu-Al-Ni alloys have been studied by many workers.[1–13] These studies have shown that when an alloy with a chemical composition in the range of Cu-(14 to 15.1) wt pct Al-(3.1 to 4.3) wt pct Ni was solution-heat-treated at a point in the single β phase (disordered body-centered cubic) region and then quenched into room-temperature water or iced-brine, the microstructure was single $D0_3$ phase,[1–4] or $D0_3$ phase containing extremely fine precipitates.[5,6] By using the electron diffraction method, the crystal structure of the extremely fine precipitates was determined to be of the 2H type.[5,6,7] When the as-quenched alloy was aged at temperatures ranging from 450 °C to 550 °C for moderate times and then quenched, γ_2 particles started to precipitate within the $D0_3$ matrix at the aging temperature and the remaining $D0_3$ matrix would transform to γ_1' martensite during quenching.[7,8] With increasing the aging time within this temperature range, fine B2 precipitates were found to occur within the well-grown γ_2 particles and the remaining $D0_3$ matrix would completely transform to α phase (disordered face-centered cubic) or a mixture of ($\alpha + \beta$) phases at the aging temperature.[7,8,9]

Recently, we have performed transmission electron microscopy examinations on the phase transformations of the Cu-14.2 wt pct Al-7.8 wt pct Ni alloy. Consequently, we found that in the as-quenched condition, the microstructure of the alloy was $D0_3$ phase containing extremely fine L–J precipitates. The L–J phase has an orthorhombic structure with lattice parameters $a = 0.413$ nm, $b = 0.254$ nm, and $c = 0.728$ nm, which was first found and identified by the present workers in a $Cu_{2.2}Mn_{0.8}Al$ alloy.[14] This result is different from that reported by other workers.[5,6] In addition, when the as-quenched alloy was aged at 500 °C for a long time, the B2 precipitates could be observed not only within the γ_2 particles but also within the α phase. This feature has never been observed by other workers in the Cu-Al-Ni alloys.

C.H. CHEN, Graduate Student, Department of Materials Science and Engineering, and T.F. LIU, Professor and Dean of the College of Engineering, are with the National Chiao Tung University, Hsinchu, Taiwan, Republic of China. Contact e-mail address: andychen.mse86g@nctu.edu.tw

Manuscript submitted February 12, 2002.

II. EXPERIMENTAL PROCEDURE

The alloy, Cu-14.2 wt pct Al-7.8 wt pct Ni (Cu-28.0 at. pct Al-7.0 at. pct Ni), was prepared in a vacuum induction furnace by using 99.9 pct copper, 99.9 pct aluminum, and 99.9 pct nickel. The melt was chill cast into a 30 × 50 × 200-mm copper mold. After being homogenized at 1000 °C for 72 hours, the ingot was sectioned into 2.0-mm-thick slices. These slices were subsequently solution-heat-treated at 1000 °C for 1 hour and then quenched into iced-brine. The aging processes were performed at 500 °C for various times in a vacuum-heat-treated furnace.

Electron microscopy specimens were prepared by means of a double-jet electropolisher with an electrolyte of 70 pct methanol and 30 pct nitric acid. The polishing temperature was kept in the range from −40 °C to −20 °C, and the current density was kept in the range from 3.0×10^4 to 6.0×10^4 A/m^2. Electron microscopy was performed on a JEOL* JEM-2000FX scanning transmission electron microscope (TEM) operating at 200 kV. This microscope was equipped with a Link** ISIS 300 energy-dispersive X-ray spectrometer (EDS) for chemical analysis. Quantitative analyses of elemental concentrations for Cu, Al, and Ni were made with the aid of a Cliff-Lorimer Ratio Thin Section method.

*JEOL is a trademark of Japan Electron Optics Ltd., Tokyo.

**Link is a trademark of Oxford Ltd., UK.

III. RESULTS

Figure 1(a) is a bright-field (BF) electron micrograph of the as-quenched alloy, exhibiting the presence of the extremely fine precipitates with a mottled structure within the matrix. This feature is similar to that observed by other workers in the Cu-Al-Ni alloys.[5,6] Figures 1(b) through (d) show three different selected-area diffraction patterns (SADPs) of the as-quenched alloy. It is seen in these SADPs that in addition to the reflection spots corresponding to the $D0_3$ phase,[5–7,15–17] the diffraction patterns also consist of extra spots with streaks caused by the presence of the

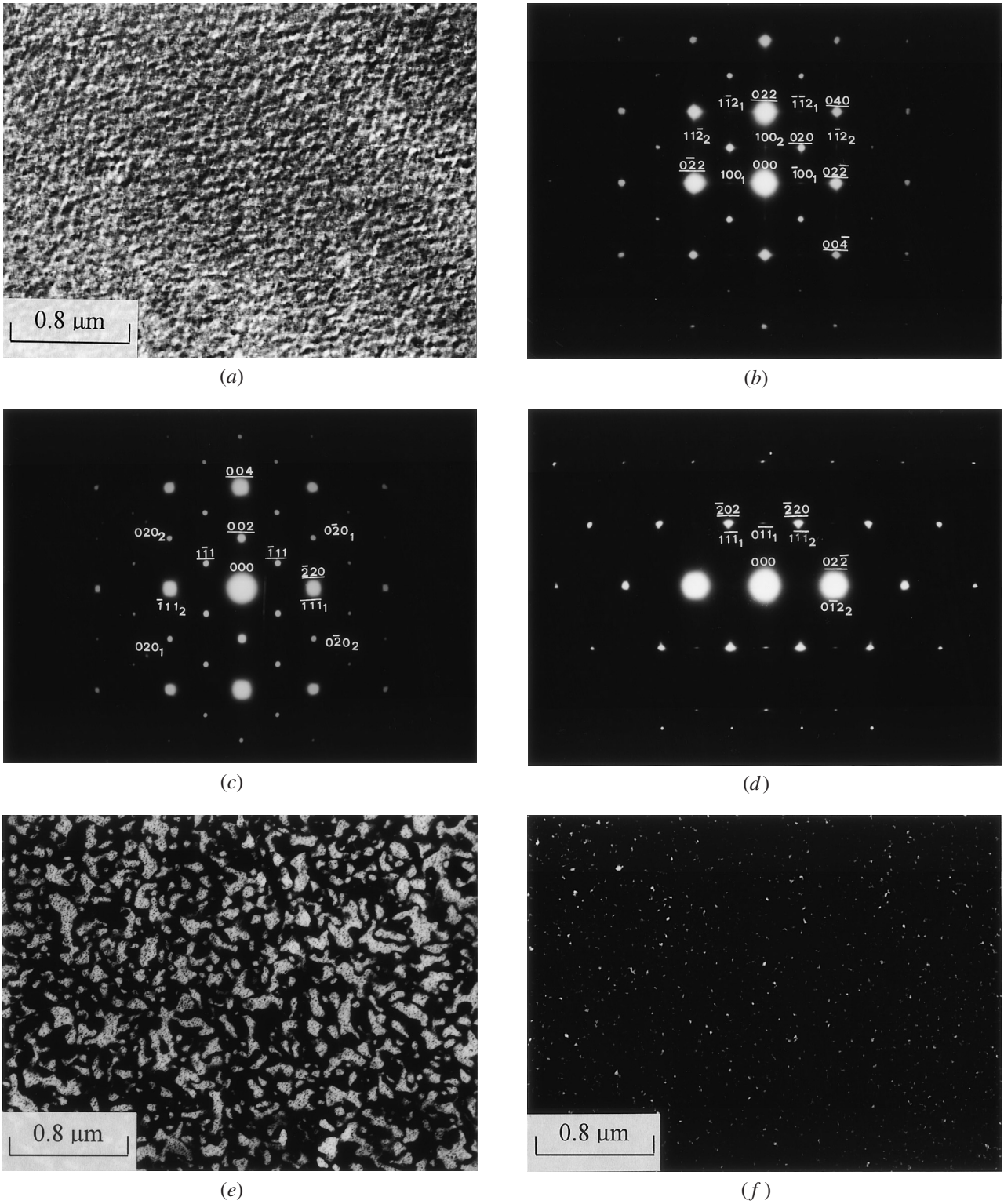

Fig. 1—Electron micrographs of the as-quenched alloy: (*a*) BF and (*b*) through (*d*) three SADPs. The zone axes of the $D0_3$ phase are (b) [100], (c) [110], and (d) [111] ($\underline{hkl}$ = $D0_3$ phase, hkl_{1or2} = L–J phase, 1: variant 1, and 2: variant 2). (*e*) ($\bar{1}11$) $D0_3$ and (*f*) L–J DF.

extremely fine precipitates. When compared with our previous studies in the Cu-14.6Al-4.3Ni and $Cu_{2.2}Mn_{0.8}Al$ alloys,[13,14] it is found that the extra spots with streaks should belong to the L–J phase with two variants, rather than the 2H phase, as reported by other workers.[5,6] Figure 1(e) is a ($\bar{1}11$) $D0_3$ dark-field (DF) electron micrograph of the same area as Figure 1(a), revealing the presence of the $D0_3$ domains. In this figure, it is also seen that a high density of the extremely fine L–J precipitates (dark contrast) was present within the $D0_3$ domains. Figure 1(f), a (100_1) L–J DF electron micrograph, exhibits the presence of the extremely fine L–J precipitates. Based on the preceding observations, it is concluded that the as-quenched microstructure of the alloy was $D0_3$ phase containing extremely fine L–J precipitates.

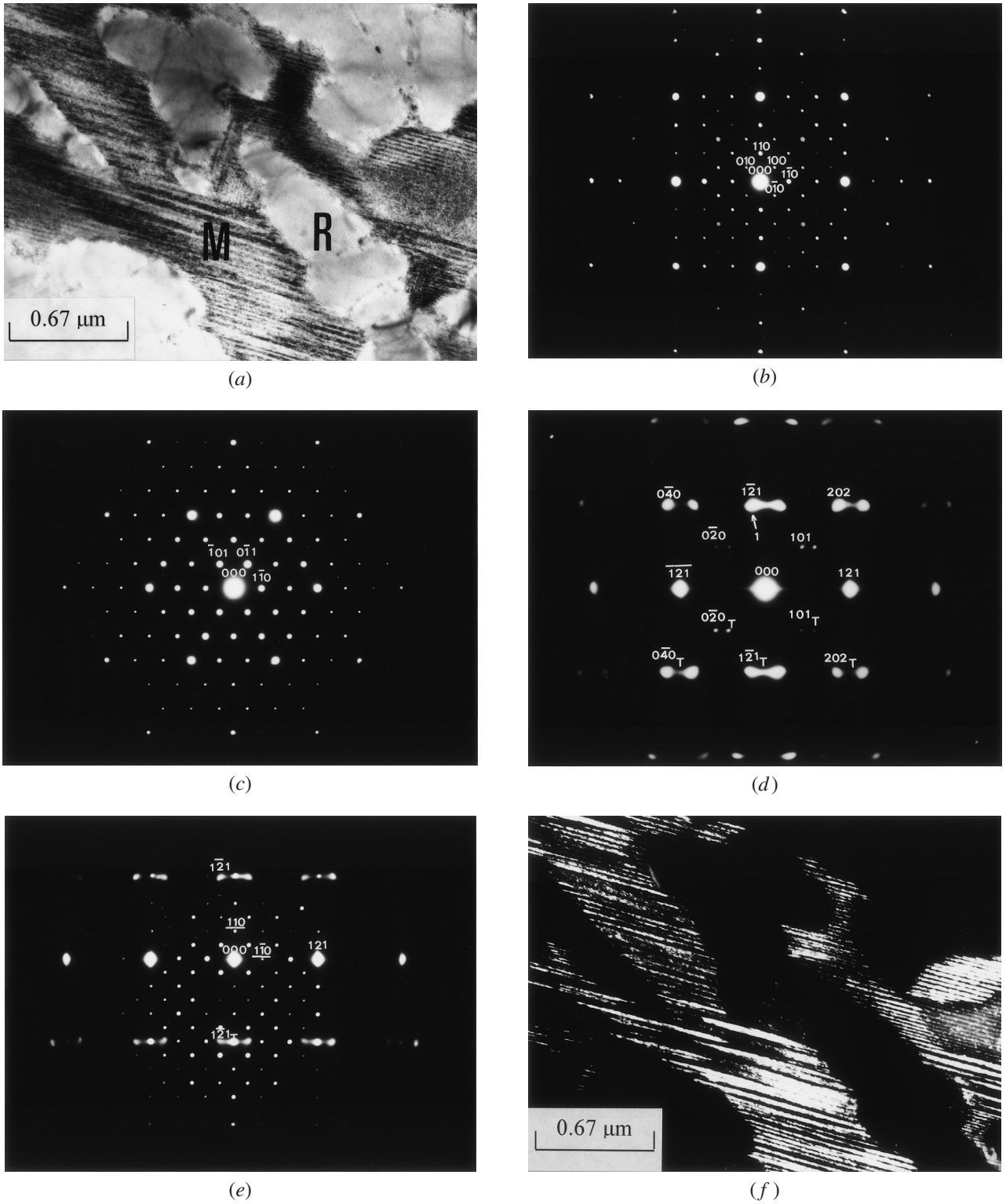

Fig. 2—Electron micrographs of the alloy aged at 500 °C for 5 min: (*a*) BF and (*b*) and (*c*) two SADPs taken from the precipitate marked as "R" in (a). The zone axes of the γ_2 particle are (b) [001] and (c) [111]. (*d*) An SADP taken from the precipitate marked as "M" in (a). The zone axis of the γ_1' martensite is [10$\bar{1}$]. (*e*) An SADP taken from a γ_2 particle and its surrounding γ_1' martensite. The zone axes of the γ_2 particle, γ_1' martensite, and internal twin are [001], [10$\bar{1}$], and [$\bar{1}$01], respectively ($\underline{hkl}$ = γ_2 phase, hkl = γ_1' martensite, and hkl_T = internal twin). (*f*) (12$\bar{1}$) γ_1' DF.

When the as-quenched alloy was aged at 500 °C for 5 minutes and then quenched, both the $D0_3$ and L–J phases could not be observed and the other two kinds of phases started to occur, as illustrated in Figure 2(a). Figures 2(b) and (c), two SADPs taken from the precipitate marked as "R" in Figure 2(a), indicate that the precipitate has an ordered body-centered cubic structure with lattice parameter a = 0.872 nm, which is consistent with that of the γ_2 phase.[1,8] Figure 2(d) is an SADP taken from an area marked as "M" in Figure 2(a). When compared with the previous study in

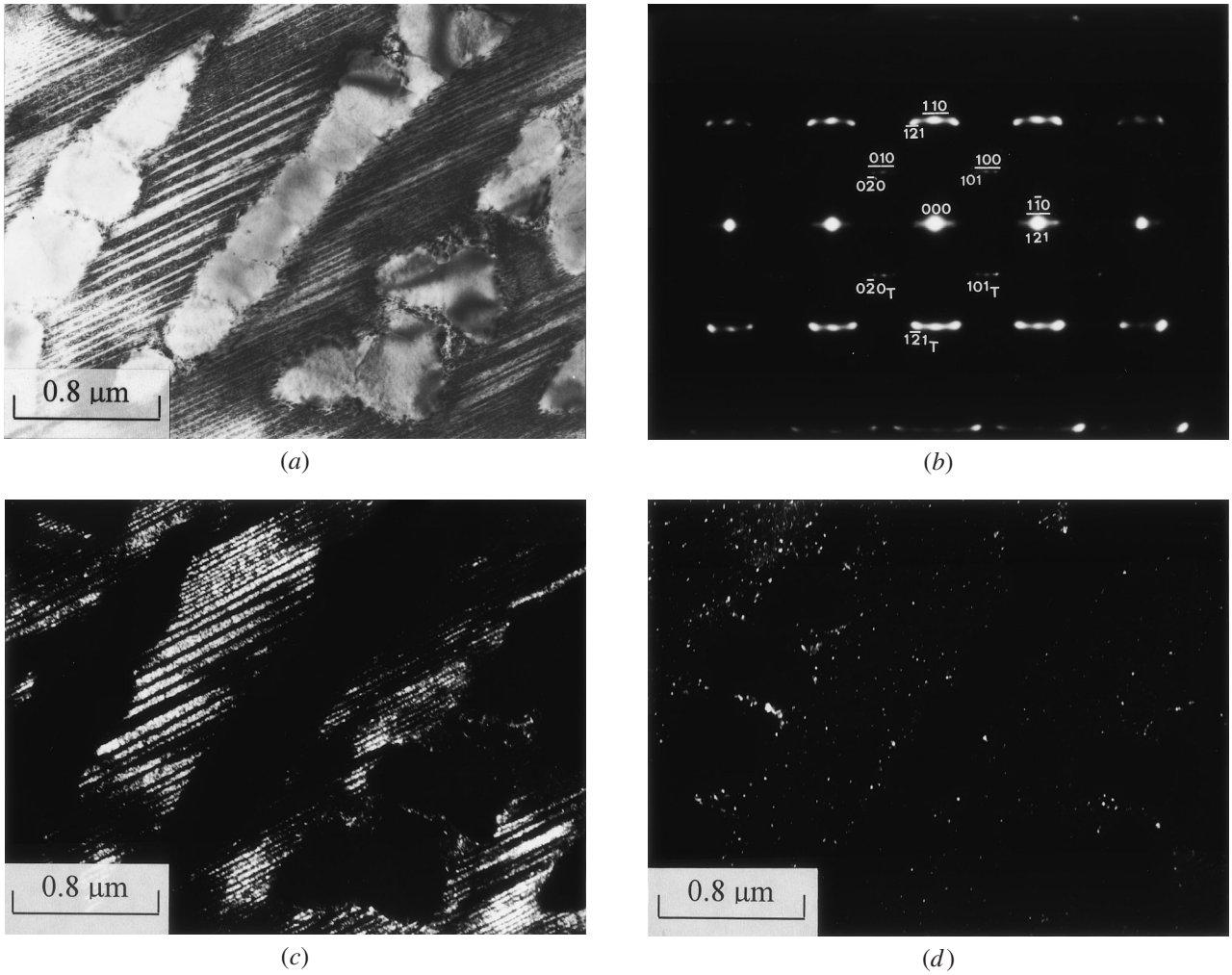

Fig. 3—Electron micrographs of the alloy aged at 500 °C for 10 min: (*a*) BF and (*b*) an SADP. The zone axes of the B2 phase, γ_1' martensite, and internal twin are [001], [10$\bar{1}$], and [101], respectively ($\underline{hkl}$ = B2 phase, hkl = γ_1' martensite, and hkl_T = internal twin). (*c*) (1$\bar{2}$1) γ_1' and (*d*) (100) B2 DF, respectively.

the Cu-Al-Ni alloy,[2] it is found that the positions and streak behaviors of the reflection spots are the same as those of the γ_1' martensite with internal twins. The γ_1' martensite has an orthorhombic structure with lattice parameters a = 0.440 nm, b = 0.534 nm, and c = 0.422 nm.[1] Shown in Figure 2(e) is an SADP taken from a γ_2 particle and its surrounding γ_1' martensite, indicating that the orientation relationship between the γ_2 particle and the γ_1' martensite is $(1\bar{1}0)_{\gamma_2}//(121)_{\gamma_1'}$ and $[001]_{\gamma_2}//[10\bar{1}]_{\gamma_1'}$. Figure 2(f), a DF electron micrograph taken with the reflection spot marked as "1" in Figure 2(d), clearly reveals the presence of the γ_1' martensite with a lamellar structure. In the previous studies,[3,7,10] it was reported that when the Cu-14Al-4Ni alloy was aged at 450 °C for short times and then cooled to 160 °C, the $D0_3 \rightarrow \gamma_1'$ martensitic transformation would occur during cooling, and the increase of either aluminum or nickel content would lower the martensitic transformation temperature. In the present alloy, the aluminum content is similar to that of the Cu-14Al-4Ni alloy and the nickel content is obviously higher. Therefore, it is reasonable to believe that the γ_1' martensite present in Figure 2(a) should be formed through a $D0_3 \rightarrow \gamma_1'$ martensitic transformation during quenching from the aging temperature, rather than at the aging temperature.

Figure 3(a) shows a BF electron micrograph of the alloy aged at 500 °C for 10 minutes and then quenched, revealing the presence of the γ_2 particles and the γ_1' lamellar martensite. This feature is similar to that observed in Figure 2(a). Therefore, it is likely to deduce that the microstructure of the alloy isothermally held at 500 °C for 10 minutes was still the mixture of ($D0_3$ + γ_2) phases. However, electron diffraction examinations of the lamellar structure indicated that in addition to the reflection spots of the γ_1' martensite with internal twins, some faint reflection spots corresponding to the B2 phase could be detected. A typical SADP is shown in Figure 3(b). Figures 3(c) and (d), (1$\bar{2}$1)γ_1' and (100) B2 DF electron micrographs, clearly exhibit the presence of the γ_1' martensite and the extremely fine B2 precipitates, respectively. In Figure 3(d), it is also seen that when the alloy was aged at 500 °C for short times, the B2 precipitates were only formed within the $D0_3$ matrix and no evidence of the B2 precipitates could be detected within the γ_2 particles. Figures 4(a) and (b) are BF and (100) B2 DF electron micrographs of the alloy aged at 500 °C for 30 minutes and then quenched, revealing that the size of the B2 precipitates increased with increasing the aging time and the remaining $D0_3$ matrix transformed to the α phase completely.

Figure 4(c), an SADP taken from an area covering the

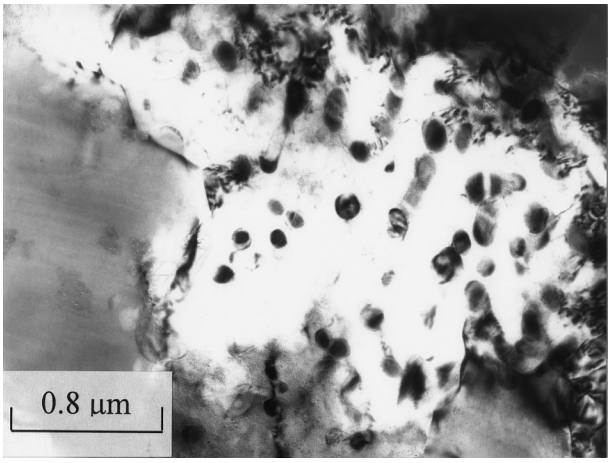

(*a*)

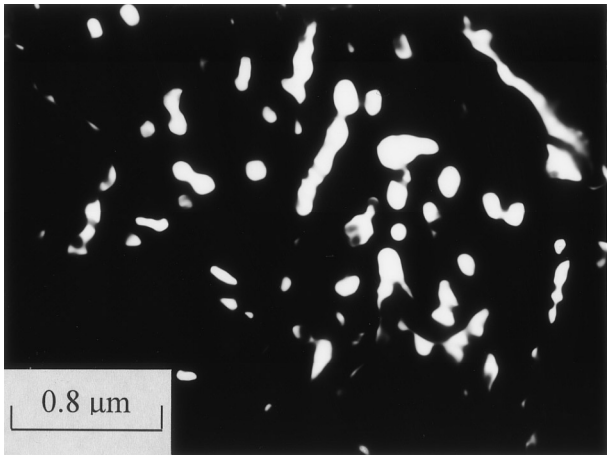

(*b*)

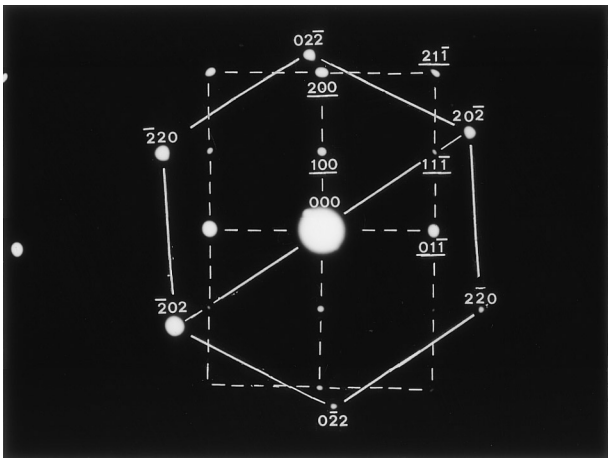

(*c*)

Fig. 4—Electron micrographs of the alloy aged at 500 °C for 30 min: (*a*) BF, (*b*) (100) B2 DF, and (*c*) an SADP taken from an area covering the B2 precipitates and their surrounding α matrix. The zone axes of the B2 precipitate and α phase are [011] and [111], respectively ($\underline{hkl}$ = B2 phase, and hkl = α phase).

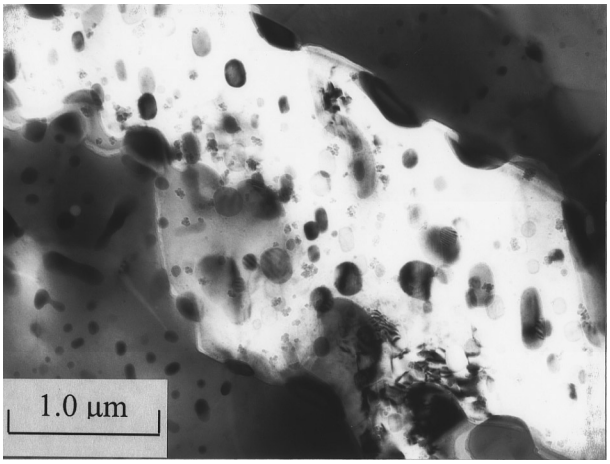

(*a*)

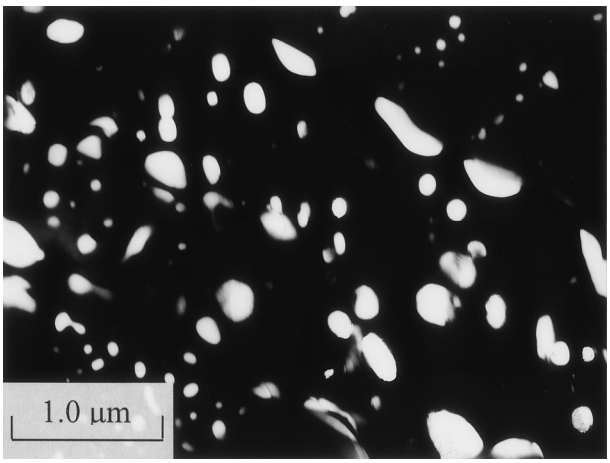

(*b*)

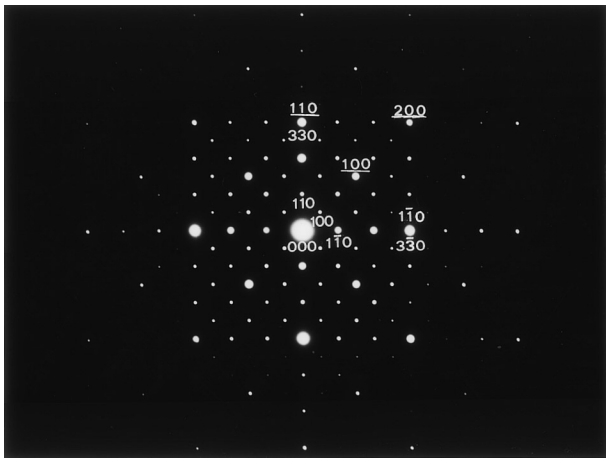

(*c*)

Fig. 5—Electron micrographs of the alloy aged at 500 °C for 3 h: (*a*) BF, (*b*) (100) B2 DF, and (*c*) an SADP taken from an area covering the B2 precipitates and their surrounding γ_2 matrix. The zone axes of the B2 precipitate and γ_2 matrix are [001] and [001], respectively ($\underline{hkl}$ = B2 phase, and hkl = γ_2 phase).

B2 precipitates and their surrounding α matrix, indicates that the orientation relationship between the B2 precipitate and the α phase is $(11\bar{1})_{B2}//(10\bar{1})_{\alpha}$ and $[011]_{B2}//[111]_{\alpha}$, which corresponds to the Kurdjumov–Sachs orientation relationship. Transmission electron microscopy examinations revealed that when the alloy was aged at 500 °C for less than 60 minutes, the B2 precipitates were only formed within the α phase and not within the γ_2 particles. However, pro-

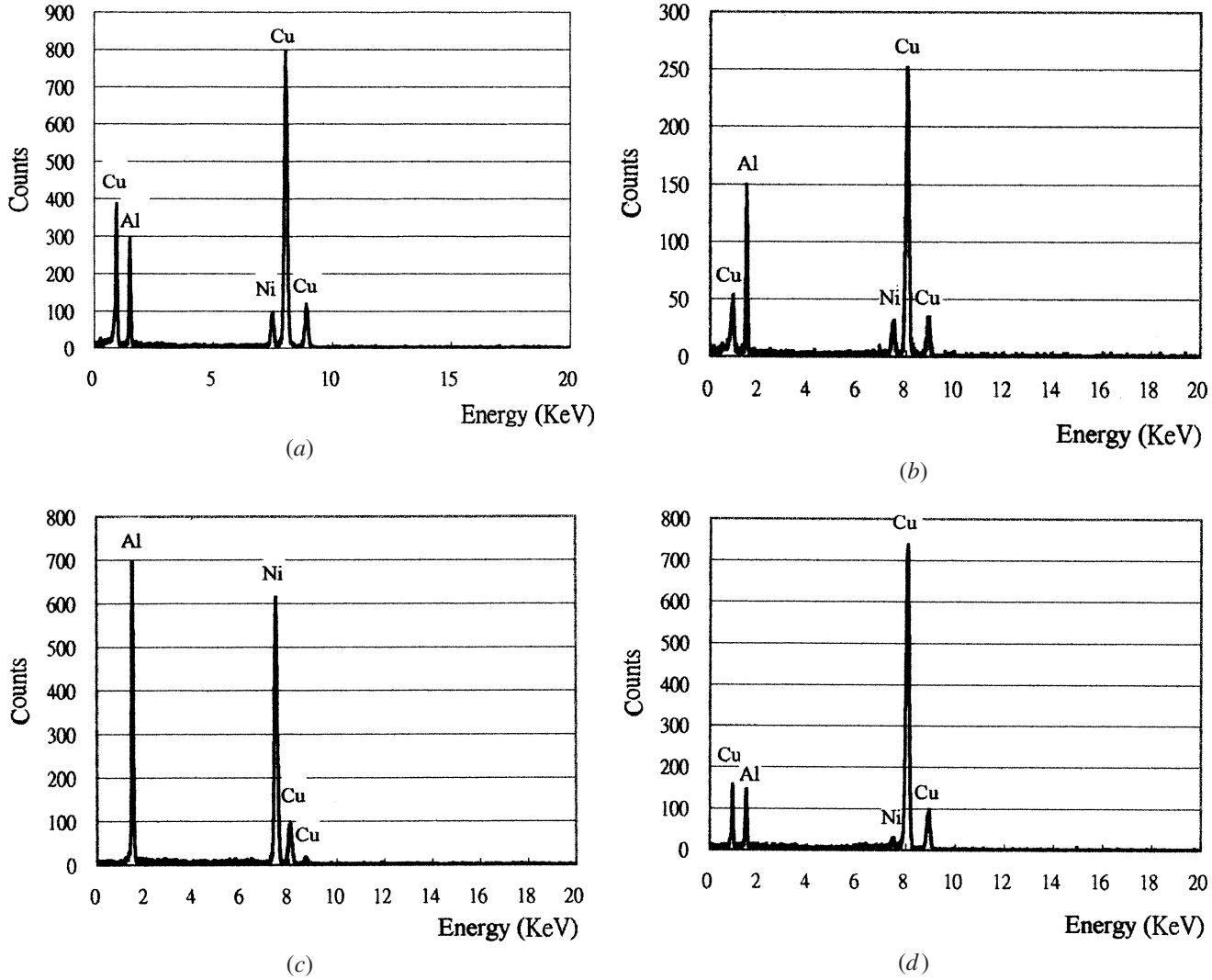

Fig. 6—Four typical EDS spectra obtained from (*a*) as-quenched alloy, and (*b*) a γ_2 particle, (*c*) a B2 precipitate, as well as (*d*) α phase in the alloy aged at 500 °C for 30 min.

longed aging at the same temperature caused the B2 precipitates started to appear within the γ_2 particles. A typical microstructure is shown in Figure 5(a). Figure 5(b) is a (100) B2 DF electron micrograph of the same area as in Figure 5(a), showing that the size of the B2 precipitates at the α/γ_2 interface and within the α phase is greater than that within the γ_2 particles. Figure 5(c), an SADP taken from an area covering the B2 precipitates and their surrounding γ_2 matrix, indicates that the orientation relationship between the B2 precipitate and the γ_2 matrix is cubic to cubic. This result is similar to that observed by other workers in the aged Cu-Al-Ni alloys.[11]

IV. DISCUSSION

On the basis of the preceding results, it is obvious that when the present alloy was aged at 500 °C for longer times, the remaining $D0_3$ matrix would transform to the mixture of (B2 + α) phases. This result is quite different from the mixture of (β + α) phases found by other workers in the Cu-14Al-4Ni alloy aged at 500 °C or 550 °C.[7,9] In order to clarify the apparent difference, an STEM-EDS study was undertaken. Figures 6(a) through (d) represent four typical EDS spectra taken from the as-quenched alloy, a γ_2 particle, a B2 precipitate (within the α phase), as well as the α phase in the alloy aged at 500 °C for 30 minutes, respectively. The average weight percentages of the alloying elements examined by analyzing at least ten different EDS spectra of each phase are listed in Table I. It is clearly seen in Figure 6 and Table I that the concentration of aluminum in the γ_2 particle is much greater than that in the as-quenched alloy, and the reverse result is obtained for the concentration of nickel. This result is similar to that examined by other workers in the Cu-14Al-4Ni alloy.[7,8,9] In their studies, they proposed that compared with the as-quenched alloy, the γ_2 particle was comparatively richer in aluminum atoms; therefore, the precipitation of the γ_2 particles had caused the martensitic transformation temperature of the remaining $D0_3$ matrix to be higher, which induced the $D0_3 \rightarrow \gamma_1'$ martensitic transformation would occur during quenching from the aging temperature. Obviously, their proposition is consistent with the observation in Figure 2(a). In addition, along with the growth of the γ_2 particles, the nickel concentration in the remaining $D0_3$ matrix would be increased with increasing the aging time. The EDS examinations revealed that when

Table I. Chemical Compositions of the Phases Revealed by an EDS

Heat Treatment	Phase	Chemical Composition (Wt Pct)		
		Cu	Al	Ni
As-quenched	$D0_3$ + L–J	77.82	14.23	7.98
500 °C 5 min	γ_2 phase	74.69	18.06	7.25
	γ_1' martensite (remaining $D0_3$ phase)	78.80	11.98	9.22
500 °C 30 min	γ_2 phase	73.88	19.21	6.91
	B2 phase	9.14	33.88	56.98
	α phase	90.17	7.87	1.96

the present alloy was aged at 500 °C for 5 minutes, the nickel concentration in the remaining $D0_3$ matrix was increased up to 9.22 wt pct (Table I), which is distinctly higher than that found by other workers in the Cu-14Al-4Ni alloy.[7] In our previous study,[18] we have demonstrated that the nickel addition in an Fe-23.2 at. pct Al alloy could pronouncedly enhance the formation of the B2 phase. Similarly, it is plausible to suggest that in the present alloy, the higher nickel concentration in the remaining $D0_3$ matrix should be favorable for the formation of the B2 precipitates, instead of the β phase observed by other workers in the Cu-14Al-4Ni alloy.[7,9] Furthermore, since the aluminum and nickel concentrations in the B2 precipitates are very high, it is thus expected that along with the growth of the B2 precipitates, the surrounding $D0_3$ matrix would be depleted in both aluminum and nickel. The lower concentration of aluminum would cause the $D0_3$ matrix to become unstable.[7,19] Consequently, the remaining $D0_3$ matrix would transform to the Cu-rich α phase.[19] This result is consistent with the observation in Figure 4(a).

Finally, one more feature is worthy of note. In the previous study,[8] it was found that the B2 precipitates formed within the γ_2 particles had a platelike shape. In the present study, however, the B2 precipitates had a granular shape. The reason why the morphology of the B2 precipitates had this difference is unclear.

V. CONCLUSIONS

The as-quenched microstructure of the Cu-14.2Al-7.8Ni alloy was $D0_3$ phase containing extremely fine L–J precipitates. When the alloy was aged at 500 °C for a short time and then quenched, γ_2 particles were formed within the $D0_3$ matrix at the aging temperature and the remaining $D0_3$ matrix underwent a $D0_3 \rightarrow \gamma_1'$ martensitic transformation during quenching. With slightly increasing aging time at the same temperature, extremely fine B2 precipitates started to occur within the remaining $D0_3$ matrix. The size of the B2 precipitates increased with increasing the aging time. Along with the growth of the B2 precipitates, the remaining $D0_3$ matrix would transform to the α phase. When the alloy was aged at 500 °C for longer times, the B2 precipitates could be observed not only within the α phase but also within the γ_2 particles.

ACKNOWLEDGMENTS

The author is pleased to acknowledge the financial support of this research by the National Science Council, Republic of China, under Grant No. NSC90-2216-E-009-044. He is also grateful to M.H. Lin for typing.

REFERENCES

1. M.A. Dvorack, N. Kuwano, S. Polat, H. Chen and C.M. Wayman: *Scripta Metall.*, 1983, vol. 17, pp. 1333-36.
2. N. Kuwano and C.M. Wayman: *Metall. Trans. A*, 1984, vol. 15A, pp. 621-26.
3. N.F. Kennon, D.P. Dunne, and L. Middleton: *Metall. Trans. A*, 1982, vol. 13A, pp. 551-55.
4. N. Zárubová, A. Gemperle, and V. Novák: *Mater. Sci. Eng. A*, 1997, vol. A222, pp. 166-74.
5. K. Otsuka, H. Sakamoto, and K. Shimizu: *Trans. JIM*, 1979, vol. 20, pp. 244-54.
6. K. Otsuka, H. Kubo, and C.M. Wayman: *Metall. Trans. A*, 1981, vol. 12A, pp. 595-605.
7. J. Singh, H. Chen, and C.M. Wayman: *Metall. Trans. A*, 1986, vol. 17A, pp. 65-72.
8. J. Singh, H. Chen, and C.M. Wayman: *Scripta Metall.*, 1985, vol. 19, pp. 887-90.
9. J. Singh, H. Chen, and C.M. Wayman: *Scripta Metall.*, 1985, vol. 19, pp. 231-34.
10. V. Agafonov, P. Naudot, A. Dubertret, and B. Dubois: *Scripta Metall.*, 1988, vol. 22, pp. 489-94.
11. Y.S. Sun, G.W. Lorimer, and N. Ridley: *Metall. Trans. A*, 1990, vol. 21A, pp. 575-88.
12. J. Tan and T.F. Liu: *Scripta Mater.*, 2000, vol. 43, pp. 1083-88.
13. J. Tan and T.F. Liu: *Mater. Chem. Phys.*, 2001, vol. 70, pp. 49-53.
14. S.C. Jeng and T.F. Liu: *Metall. Mater. Trans. A*, 1995, vol. 26A, pp. 1353-65.
15. T.F. Liu, G.C. Uen, C.Y. Chao, Y.L. Lin, and C.C. Wu: *Metall. Trans. A*, 1991, vol. 22A, pp. 1407-15.
16. C.C. Wu, J.S. Chou, and T.F. Liu: *Metall. Trans. A*, 1990, vol. 22A, pp. 2265-76.
17. K.C. Chu, S.C. Jeng, and T.F. Liu: *Scripta Metall.*, 1996, vol. 34, pp. 83-87.
18. T.F. Liu, S.C. Jeng, and C.C. Wu: *Metall. Trans. A*, 1992, vol. 23A, pp. 1395-1401.
19. X.J. Liu, I. Ohnuma, R. Kainuma, and K. Ishida: *J. Alloys Compounds*, 1998, vol. 264, pp. 201-08.